Available online at www.sciencedirect.com
ScienceDirect
Journal of Non-Crystalline Solids 354 (2008) 503–508
JOURNAL OF NON-CRYSTALLINE SOLIDS
www.elsevier.com/locate/jnoncrysol

Optical properties of amorphous $(As_{0.33}S_{0.67})_{100-x}Te_x$ ($x = 0$, 1, 5 and 10) chalcogenide thin films, photodoped step-by-step with silver

E. Márquez [a,*], J.M. González-Leal [a], A.M. Bernal-Oliva [a], R. Jiménez-Garay [a], T. Wagner [b]

[a] Departamento de Física de la Materia Condensada, Facultad de Ciencias, Universidad de Cádiz, Campus de Puerto Real, 11510 Puerto Real (Cádiz), Andalucía, Spain
[b] Department of General and Inorganic Chemistry, University of Pardubice, 53210 Pardubice, Czech Republic

Available online 31 October 2007

Abstract

We have analysed in detail the effect of silver-content on the optical properties of Ag-photodoped amorphous $(As_{0.33}S_{0.67})_{100-x}Te_x$ (with $x = 0$, 1, 5 and 10 at.%) chalcogenide thin films; the chalcogenide host layers were prepared by vacuum thermal evaporation. Films of composition $Ag_y[(As_{0.33}S_{0.67})_{100-x}Te_x]_{100-y}$, with $y \lesssim 18$ at.%, were successfully obtained by successively photodissolving about 20- or 40-nm-thick layers of silver. The optical constants (n,k) have been accurately determined by an improved envelope method [J.M. González-Leal, R. Prieto-Alcón, J.A. Angel, D.A. Minkov, E. Márquez, Appl. Opt. 41 (2002) 7300], based on the two envelope curves of the optical-transmission spectrum, obtained at normal incidence. The dispersion of the refractive index of the Ag-photodoped chalcogenide films is analysed in terms of the Wemple–DiDomenico single-effective-oscillator model: $n^2(\hbar\omega) = 1 - E_o E_d/(E_o^2 - (\hbar\omega)^2)$, where E_o is the single-oscillator energy, and E_d the dispersion energy. We found that the refractive index of the Ag-doped samples strongly increases with the Ag-content, whereas the optical band gap, E_g^{opt}, decreases also notably. For instance, in the particular case of $x = 10$ at.%, the largest Te-content, E_g^{opt} decreases from 2.17 down to 1.67 eV. It should also be mentioned that, in the case of the undoped samples, when the Te-concentration increases from zero up to 10 at.%, the value of E_g^{opt} decreases from 2.49 down to 2.17 eV.

PACS: 78.20.Ci; 78.66.Jg

Keywords: Amorphous semiconductors; Optical spectroscopy; Photo-induced effects

1. Introduction

The light-induced solid-state chemical reaction between various metals (Ag, Cu, Zn and Cd), and chalcogenide glasses (also known as 'photodiffusion', 'photodoping' or 'photodissolution'), has been widely studied [1–6]. However, at present, the mechanism for this photo-induced phenomenon is still speculative to our knowledge. Silver-doped chalcogenide glasses have been investigated mainly for their potential applications as optical recording materials, and more recently, as materials for diffractive optics and optical integrated circuits for IR operation [7,8]. All these important applications require the fabrication of structures in a range of thicknesses, from one to tenths of a micron. Understanding of the kinetics of the metal photodissolution effect, and finding new, suitable host glass-matrices, is certainly crucial points for the above-mentioned technological applications.

In the present paper, we have analysed in detail the influence of 'room-temperature, step-by-step Ag-photodoping', on the optical properties of amorphous $(As_{0.33}S_{0.67})_{100-x}Te_x$ (with $x = 0$, 1, 5 and 10 at.%) ternary chalcogenide films. In a previous paper [9], we have

* Corresponding author. Tel.: +34 956 016318; fax: +34 956 016288.
E-mail address: emilio.marquez@uca.es (E. Márquez).

0022-3093/$ - see front matter © 2007 Elsevier B.V. All rights reserved.
doi:10.1016/j.jnoncrysol.2007.06.087

reported on the behaviors of the refractive index and absorption coefficient, and also on the structure, of the corresponding undoped As–S–Te chalcogenide samples. We believe that this is the first time that a systematic optical characterization of Ag–As–S–Te quaternary alloy films is presented.

2. Experimental

Chalcogenide host thin films were deposited using the vacuum thermal evaporation technique. First, to produce the bulk glass for the evaporation source, the constituents were measured into a quartz tube, vacuum-sealed, and melted in a rocking furnace for 24 h at 920 °C, and, subsequently, quenched in air. Fragments of the bulk material were then used to prepare the films in a vacuum chamber with a pressure of approximately 1×10^{-6} Torr, and at a rate of 1 nm s^{-1} (the deposition rate was continuously measured by the dynamical weighing procedure). X-ray diffraction showed that all the films to be studied, were completely amorphous, and their chemical compositions were checked by EDX-analysis. The thicknesses of the films ranged between about 800 and 1200 nm, which are appropriate for the accurate evaluation of their optical parameters, by the *envelope* method that has been used in the present work, recently reported by González-Leal et al. [10].

Next, different layers of silver were deposited on top of the chalcogenide host. For the silver evaporation we used an Al_2O_3-covered tungsten boat, thereby reducing both the heat and light exposure of the samples, during deposition. Photodoping was carried out by illuminating the samples with a 500 W tungsten lamp, equipped with a large Fresnel lens and IR-cut filter. During light exposure, the samples were sandwiched between two other glass plates, in order to avoid surface oxidation. The Ag-concentration of our samples was $\lesssim$18 at.%. When preparing layers with a large Ag-content, we found that photodissolving a thick layer of Ag, in just one step, resulted in a photodoped product that was rather inhomogeneous. However, doping the chalcogenide host, step-by-step, by consecutively dissolving ~20- or 40-nm-thick layers, produced a homogeneous layer of good optical quality, without silver remaining on top of this layer, after completing the illumination. The silver concentrations were determined from measurements of the silver and chalcogenide layer thicknesses.

The optical-transmission spectra of the samples were measured, at normal incidence, over the 300 up to 2500 nm spectral region, by a double-beam, ratio-recording, UV/Vis/NIR computer-controlled spectrophotometer (Perkin-Elmer, model Lambda-19). The spectrophotometer was set with a slit width of 2 nm. The area of illumination over which the transmission spectra were obtained, is 1 mm × 10 mm. It should be noted that the transmission spectra of the doped thin film samples were those corresponding to homogeneous, isotropic, weakly-absorbing layers, with uniform thickness – the absence of interference-fringe shrinking in those transmission spectra is a clear evidence of the 'uniform-thickness nature' of the Ag-photodoped films [11]. Lastly, the thickness of the films was also measured by a stylus-based surface profiler (Sloan, model Dektak 3030), for the purpose of comparison with the results derived from the optical-transmission spectra.

3. Results

The transmission spectra of two representative undoped and Ag-photodoped amorphous $(As_{0.33}S_{0.67})_{100-x}Te_x$ thin film samples, are plotted in Fig. 1. Judging from these experimental results, a clear red-shift occurs in the interference-free region of the spectra, with increasing Ag-content. Such a shift, as discussed later in the paper, is a consequence of the compositional dependence of the corresponding optical band gap. Also, a notable increase in the amplitude of the interference fringes, resulting from photodoping, can be seen in Fig. 1: This unambiguously reflects an increase in the refractive index of the photodoped sample.

The values of the thickness, d, refractive index, n, and absorption coefficient, α, of all the films subjected to study have been determined *only* from their normal-incidence transmission spectra, using the previously mentioned, improved envelope method, that, interestingly, takes into account the slight absorption in the glass substrate (whose

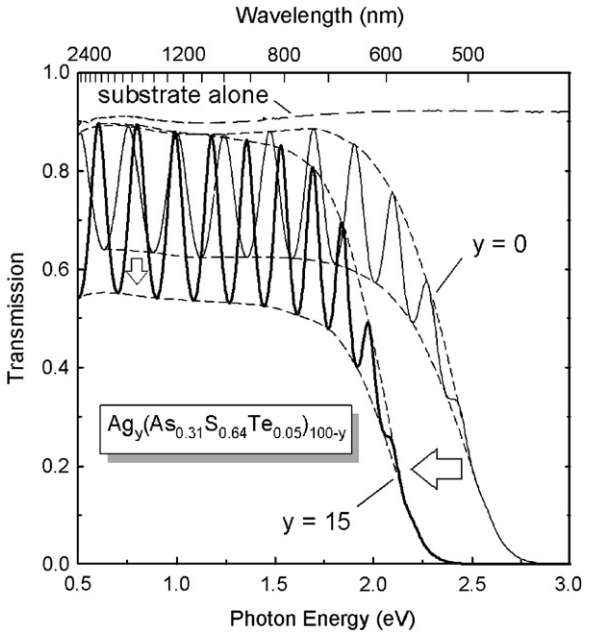

Fig. 1. Optical-transmission spectra at normal incidence of two representative undoped and Ag-photodoped amorphous $As_{31}S_{64}Te_5$ films, deposited onto *slightly-absorbing*, 1-mm-thick, borosilicate glass substrates (Menzel-Gläser microscope slides). The transmission spectrum of the bare substrate is also plotted in the graph. The top and bottom envelope curves have been computer drawn using the useful algorithm developed by McClain et al. [12].

Table 1
Initial and final thicknesses corresponding to the different amorphous $(As_{0.33}S_{0.67})_{100-x}Te_x$ chalcogenide films, after finishing with the Ag-photodissolution process

Te-content (at.%)	Undoped sample thickness, $d^{initial}_{As\text{-}S\text{-}Te}$ (nm)	Number of Ag layers (thicknesses, in nm)	Accumulated silver thickness, $d^{accumulated}_{Ag}$ (nm)	Maximum Ag-content (at.%)	$d^{initial}_{As\text{-}S\text{-}Te} + d^{accumulated}_{Ag}$ (nm)	Photodoped sample thickness, $d^{initial}_{Ag\text{-}As\text{-}S\text{-}Te}$ (nm)	Thickness contraction (%)
0	948 ± 6 (0.6%)	**4** (20, 40, 40 and 20)	120	15.93	1068	1003 ± 17 (1.7%)	6.1
1	863 ± 9 (1.0%)	**6** (all 20)	120	17.57	983	963 ± 7 (0.7%)	2.0
5	1062 ± 12 (1.1%)	**4** (20, 40, 40 and 20)	120	15.03	1182	1178 ± 9 (0.8%)	0.4
10	1182 ± 8 (0.7%)	**3** (20, 40 and 40)	100	7.46	1282	1280 ± 10 (0.8%)	0.2

Also, the number of 'Ag-photodoping steps', the accumulated Ag thickness, the final Ag-concentration, and the thickness contraction of the samples under investigation.

wavelength-dependent refractive index is around 1.5), in such a fashion that film-thickness values, with accuracies better than 2%, have been generally obtained – see Table 1 in Ref. [10], where more detailed information about the accuracy of the film-thicknesses can be found. Film-thickness results are all listed in Table 1. Alternatively, these thicknesses were directly measured by the mechanical profilometer, and the differences between the mechanically-measured and the optically-calculated values were, in all the cases, less than 3%. In addition, it is necessary to clarify that the small loss in transmission in the long-wavelength region of the spectra (see Fig. 1), is the result of an equally small surface roughness, practically 'undetectable' with the optical-characterization method employed in this work [9].

Returning to Table 1, it should be noted that the photodoped-film-thickness values clearly show that the final sample thickness, once the highest Ag-concentration has been reached, $d^{final}_{Ag\text{-}As\text{-}S\text{-}Te}$, is always smaller than the sum of the undoped sample thickness (initial thickness), $d^{initial}_{As\text{-}S\text{-}Te}$, and the *accumulated* Ag thickness, $d^{accumulated}_{Ag}$: $d^{final}_{Ag\text{-}As\text{-}S\text{-}Te} < d^{initial}_{As\text{-}S\text{-}Te} + d^{accumulated}_{Ag}$. Thus, for instance, for the sample of composition $As_{33}S_{67}$, the thickness changed from 948 nm, for the undoped film, up to 1003 nm, after photodissolving a total amount of 120 nm of Ag. The difference between the value of the sum, $d^{initial}_{As\text{-}S\text{-}Te} + d^{accumulated}_{Ag}$, 1068 nm, and the value of $d^{final}_{Ag\text{-}As\text{-}S\text{-}Te}$, was, therefore, 65 nm, which means a relative thickness *contraction* of 6.1%. The decrease of the Ag-photodoped product thickness has also been reported by Kawaguchi and Masui [13], in the cases of the binary compositions $Ge_{30}S_{70}$ and $As_{40}S_{60}$. Moreover, as seen in Table 1, the sample thickness contraction strongly decreases with increasing Te-content.

On the other hand, the optical-characterization method proposed by González-Leal et al. [10], provided values of the refractive index of the films, at the particular wavelengths where the transmission spectra are *tangential* to their top and bottom envelopes [11]. In addition, the spectral dependence (dispersion) of the index of refraction, in the visible and near-infrared regions, was analysed in terms of the useful Wemple–DiDomenico (WDD) model [14,15], which is, in turn, based on the single-effective-oscillator approach, and whose expression is

$$n^2(\hbar\omega) = 1 + \frac{E_o E_d}{E_o^2 - (\hbar\omega)^2}, \qquad (1)$$

where $\hbar\omega$ is the photon energy, E_o is the single-oscillator energy and E_d is the so-called dispersion energy or single-oscillator strength. Plots of the refractive-index factor $(n^2-1)^{-1}$ versus $(\hbar\omega)^2$, for some representative Ag–As–S–Te alloy films, are shown in Fig. 2, along with their corresponding least-squares straight lines. It is worth emphasizing the goodness of the fits to the large-wavelength data. The typical behavior of the dispersion of n is observed in all the cases: the experimental frequency variation in the refractive index clearly departs from that given by Eq. (1), when the photon energy approaches the optical band gap, E_g^{opt}. The values of the WDD dispersion parameters, E_o and E_d, were directly determined from the slope, $(E_o E_d)^{-1}$, and the intercept on the vertical axis, E_o/E_d, of the respective straight lines. The dependence of E_o and E_d on Ag-content, for all the samples subjected to study, are shown in Fig. 3(a) and (b); the Ag-content dependence of the static refractive index, $n(\hbar\omega = 0)$, is also displayed, in Fig. 3(c).

Once the values of the refractive index are known in the whole working spectral region, in terms of Eq. (1), the

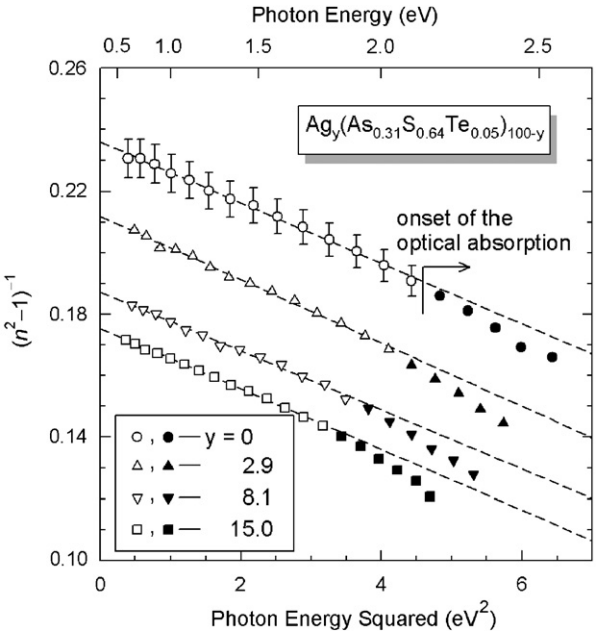

Fig. 2. WDD fits of the optical-dispersion data, corresponding to undoped and Ag-photodoped $As_{31}S_{64}Te_5$ films. Dashed straight lines are linear least-squares fits.

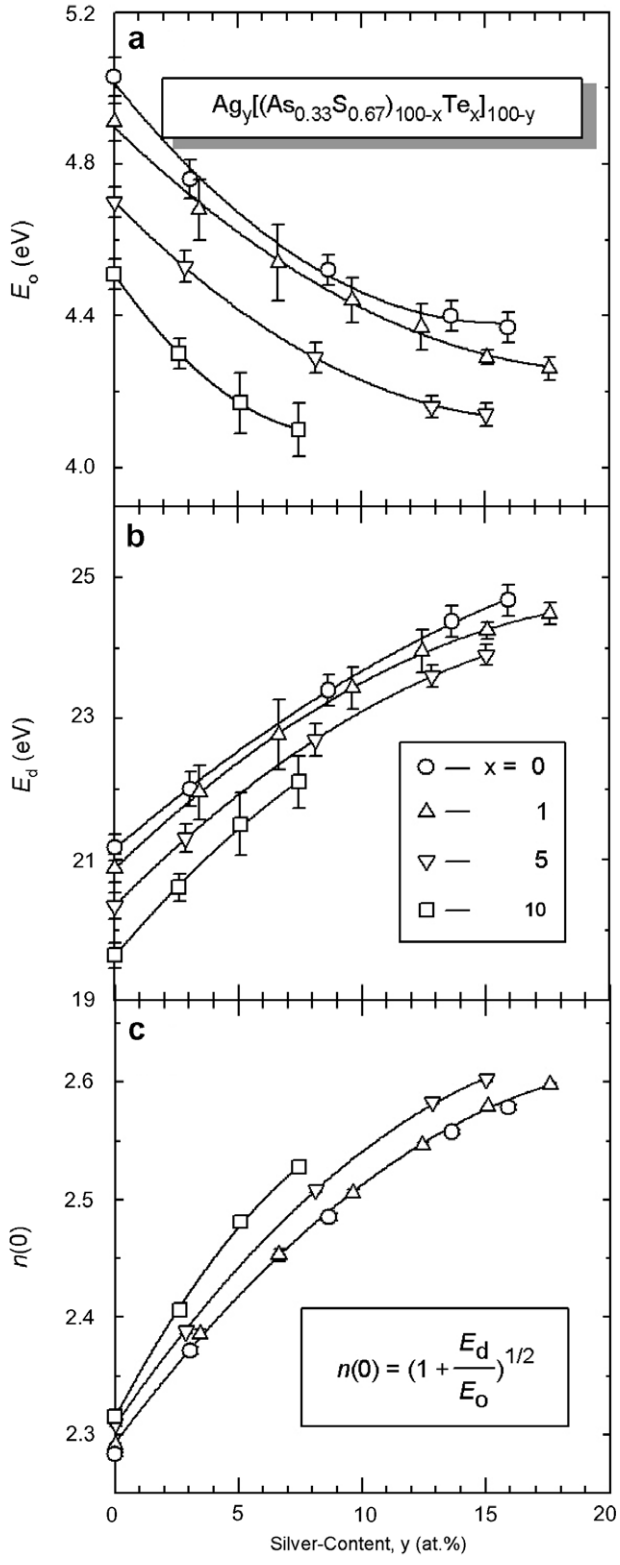

Fig. 3. Compositional dependences of the single-effective-oscillator parameters (a) E_o, and (b) E_d. Also, (c) the variation of the static refractive index, $n(\hbar\omega = 0)$, with the Ag-content, for each one of the compositions subjected to study. All the solid lines are to guide the eye.

optical-absorption spectra, $\alpha(\hbar\omega)$ the present alloy films were then derived from the *upper*, envelope of their transmission spectra [10]. Some of the calculated spectra of α

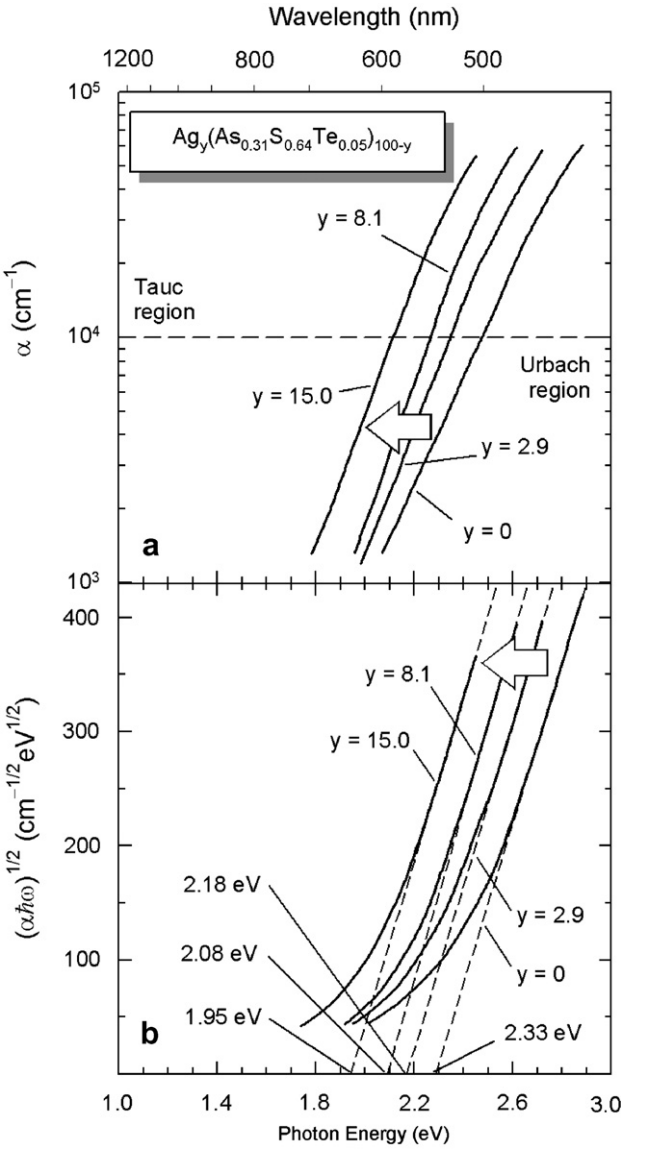

Fig. 4. (a) Optical-absorption spectra, $\alpha(\hbar\omega)$, of undoped and Ag-photodoped amorphous $As_{31}S_{64}Te_5$ films. (b) Determination of the optical band gaps in terms of Tauc's law, as linear extrapolation (dashed straight lines), of the high-energy (or high-absorption) data.

are displayed in Fig. 4(a), using a logarithmic scale: in order to complete the computation of the optical constants (n,k), the extinction coefficient, k, is easily obtained from the already-known α-values, using the basic formula, $k = \alpha\lambda/4\pi$. Next, the optical gap, E_g^{opt}, was determined from the intercept on the energy axis of the linear fit of the larger energy data, in a plot of $(\alpha\hbar\omega)^{1/2}$ versus $\hbar\omega$ (the so-called Tauc extrapolation [16]) – the associated Tauc plots are shown in Fig. 4(b). Furthermore, in Fig. 5 the dependence of the Tauc gap of Ag–As–S–Te films on Ag-content, is shown. Significant decreases of E_g^{opt} have been found in all the cases investigated, with increasing Ag-content, suggesting also notable changes occurring in the structure of the resulting photodoped material, in relation to the starting undoped material.

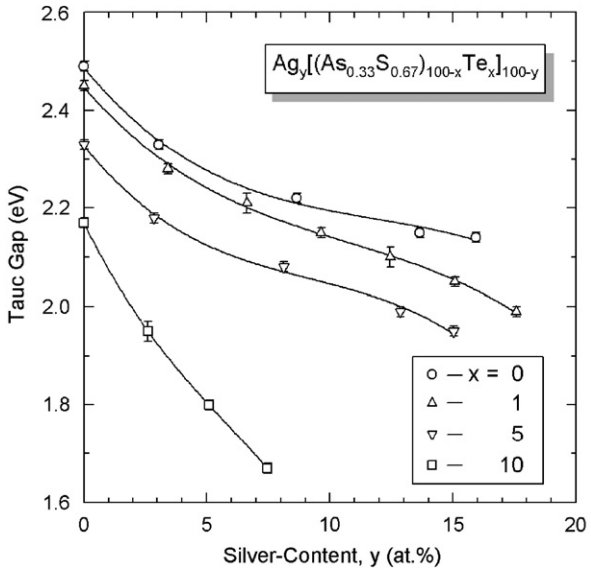

Fig. 5. Tauc gap versus Ag-content, for each one of the compositions under investigation. The solid lines are to guide the eye.

4. Discussion

In Fig. 3(a) a strong decrease is observed in the dispersion parameter, E_o, for the Ag–As–S–Te films, with increasing Ag-content. The single-oscillator energy, E_o, is considered an *average* band gap, the so-called 'WDD gap', and it corresponds to the distance between the 'centres of gravity' of the valence and conduction bands: E_o is, therefore, related to the bond energy of the different chemical bonds present in the material. Thus, the decrease observed in E_o for the films under study, is mainly due presumably to the lower bond energies of Ag–S and Ag–Te bonds, 217 and 196 kJ mol^{-1} [17], respectively, in comparison with those corresponding to S–S, S–Te and Te–Te bonds, 425, 339 and 258 kJ mol^{-1}, respectively. On the other hand, the dispersion energy, E_d, serves as a measure of the strength of interband transitions. An important achievement of the WDD model is that it relates the dispersion energy to other physical parameters of the material, through an empirical formula [14,15]

$$E_d = \beta N_c Z_a N_e \ (\text{eV}), \tag{2}$$

where β is a two-valued constant, with an 'ionic' or a 'covalent' value ($\beta_i = 0.26 \pm 0.03$ eV and $\beta_c = 0.37 \pm 0.04$ eV, respectively), N_c, the coordination of the cation nearest neighbour to the anion, Z_a, the formal chemical valency of the anion, and, N_e, the total number of valence electrons (cores excluded), per anion.

The incorporation of Ag into the structure of the present $(As_{0.33}S_{0.67})_{100-x}Te_x$ glass films has the effect of increasing the oscillator strength (see Fig. 3(b)). So, the addition of Ag into the ternary chalcogenide matrix increases one or other of the quantities on the right-hand side of Eq. (2). Even if the Ag-photodoping were to change the nature of the chemical bonding towards ionic, this cannot be the major factor, since this particular factor would decrease the parameter β. Furthermore, in ionic materials the larger s–p splitting decreases the parameter N_e – it should be pointed out here, that in the case of some Ag-containing materials, d-state core electrons of Ag atoms contribute to N_e [14,18]. Therefore, in our case of $Ag_y[(As_{0.33}S_{0.67})_{100-x}Te_x]_{100-y}$ thin film samples, it is, indeed, reasonable to assume that the average cation coordination is the factor that is most affected by the addition of Ag to the glassy structure (it must also be taken into account that $Z_a = 2$, remains valid for all the samples). This idea about the relevance of N_c is well supported by the fact that the composition of the samples at larger Ag-concentration, is relatively close to that of the ternary crystalline compound trechmannite, $AgAsS_2$, with a 25 at.% of Ag (in trechmannite, there are *four* S atoms within 3 Å of each Ag atom [19]). So, in samples with high Ag-concentrations, it might well be expected that 'structural fragments' exist, which resemble the structure of the crystalline counterpart, thus, forming a secondary phase where the silver has a higher coordination number, and, certainly, increasing the overall, average cation coordination number, N_c. We might mention here that highly-coordinated silver (with $N_{Ag} = 4$), has also been identified in other Ag-chalcogenide amorphous materials, by Fisher-Colbrie et al. [20], employing grazing-incidence X-ray scattering technique.

In the compositional dependence of the static refractive index, $n(0)$, shown in Fig. 3(c), a strong increase with increasing Ag-content, can be seen, which is justified, according to the Lorentz–Lorenz equation, by the larger electronic polarizability of the transition-metal atoms of Ag (with more easily polarizable electron clouds, and covalent radius of 153 pm), in comparison with the electronic polarizabilities of As, S and Te atoms (with covalent radii of 119, 102 and 135 pm, respectively); it must also be indicated that tellurium clearly contributes to the increase of the optical parameter $n(0)$, as it has to be expected, taking into account the impact of its relatively high covalent radius. On the other hand, a clear red-shift of the optical-absorption edge is observed in Fig. 4(a), with increasing Ag-content, for the representative sample of composition $Ag_x(As_{0.31}S_{0.64}Te_{0.05})_{100-x}$. It is stressed that following the fundamental Kramers–Kronig relationships for n and k, the red-shift in the absorption spectrum must necessarily give an increased refractive index (it is worth remembering here the relationship, $n(0) - 1 = (1/2\pi^2)\int_0^\infty \alpha \, d\lambda$), as experimentally obtained.

Finally, as can be noticed in Fig. 5, the Tauc gap decreases with the Ag-content, for all the compositions studied. This fact could be explained if we consider that, as the silver is photodoped, it, acting as a cation, joins mainly S and Te chalcogen atoms. For very low Te-contents, the incorporation of silver is expected to produce preferently the breaking of S–S homopolar bonds, which act as 'bridges' between the AsS_3 (unmixed) and AsS_2Te (mixed) pyramidal structural units, forming the structure of the material [21]. In this way, S–Ag–S linkages are created. If we now take into consideration the bond energy of

S–S bonds (425 kJ mol^{-1}), and that of Ag–S bonds (217 kJ mol^{-1}), the Ag-photodoping is obviously expected to give place to a remarkable decrease of the Tauc gap, as experimentally found. For higher Te-contents, along with the already-mentioned creation of the S–Ag–S linkages, the silver is expected presumably to also join Te atoms, yielding new Ag–Te bonds of very low bond energy (196 kJ mol^{-1}), breaking for it, both S–Te and Te–Te bonds of much larger bond energy (339 and 258 kJ mol^{-1}, respectively). Additionally, it has to be pointed out the very significant decrease of the Tauc gap, for the particular case of the composition with the highest Te-content ($x =$ 10 at.%), with increasing Ag-concentration: E_g^{opt} varies from 2.17 down to 1.67 eV, as the Ag-content changes from zero up to 7.46 at.%; that is, a decrease of 20% is found, in comparison with only the 15% decrease for the lower Te-concentrations, where the Ag-content reached is, however, about the double. Lastly, it should be emphasized that, in the case of the undoped samples, when the Te-concentration increases from zero up to 10 at.%, the value of E_g^{opt} decreases from 2.49 down to 2.17 eV.

5. Conclusion

Silver-doped amorphous $(As_{0.33}S_{0.67})_{100-x}Te_x$ (with $x = 0$, 1, 5 and 10 at.%) films, have been successfully prepared, by the room-temperature, step-by-step photodoping technique. We have analysed in detail the optical-dispersion data, using the insightful WDD single-effective-oscillator model. Dissolution of Ag into the chalcogenide matrix, introduces new Ag–S, and to a less extent, Ag–Te bonds, which clearly explains the decrease of both WDD and Tauc gaps, with increasing Ag-content. On the other hand, we attribute the increase of the oscillator strength, E_d, with the Ag-content, to the increase of the overall, effective cation coordination number, N_c, as a consequence of the formation of 'ordered regions' (i.e., a secondary phase), where the silver has a higher coordination number. The observed increase in the static refractive index, $n(0)$, with increasing Ag-concentration, is due to the corresponding increase of the WDD dispersion parameter, E_d, and to the accompanying decrease of the parameter E_o. Also, it must be stressed that Te has clearly contributed to the increase of optical parameter $n(0)$, and the decrease of E_d, E_o and E_g^{opt}. Last but not least, the maximum change in the index of refraction found in the present work, between the Ag-photodoped and undoped material (about 0.3, when the Ag-concentration reaches around 15 at.%, which means a 13% increase), makes these As–S–Te ternary chalcogenide glass films, very attractive candidates as optical recording material.

Acknowledgements

This work has been supported by the MCYT (Spain) and FEDER (EU), under FIS2005-01409 research project.

References

[1] M.T. Kostyshin, E.V. Mikhailovskaya, P.F. Romanenko, Sov. Phys.: Solid State 8 (1966) 451.
[2] A.V. Kolobov, S.R. Elliott, Adv. Phys. 40 (1991) 625.
[3] E. Márquez, R. Jiménez-Garay, A. Zakery, P.J.S. Ewen, A.E. Owen, Philos. Mag. B 63 (1991) 1169.
[4] T. Wagner, E. Márquez, J. Fernández-Peña, J.M. González-Leal, P.J.S. Ewen, S.O. Kasap, Philos. Mag. B 79 (1999) 223.
[5] E. Márquez, T. Wagner, J.M. González-Leal, A.M. Bernal-Oliva, R. Prieto-Alcón, R. Jiménez-Garay, P.J.S. Ewen, J. Non-Cryst. Solids 274 (2000) 62.
[6] T. Wagner, M. Frumar, in: A.V. Kolobov (Ed.), Photo-induced Metastability in Amorphous Semiconductors, Wiley-VCH, Weinheim, 2003, p. 160.
[7] P.J.S. Ewen, in: A.V. Kolobov (Ed.), Photo-induced Metastability in Amorphous Semiconductors, Wiley-VCH, Weinheim, 2003, p. 365.
[8] K. Richardson, T. Cardinal, M. Richardson, A. Schulte, S. Seal, in: A.V. Kolobov (Ed.), Photo-induced Metastability in Amorphous Semiconductors, Wiley-VCH, Weinheim, 2003, p. 383.
[9] E. Márquez, A.M. Bernal-Oliva, J.M. González-Leal, R. Prieto-Alcón, T. Wagner, J. Phys. D: Appl. Phys. 39 (2006) 1793.
[10] J.M. González-Leal, R. Prieto-Alcón, J.A. Angel, D.A. Minkov, E. Márquez, Appl. Opt. 41 (2002) 7300.
[11] R. Swanepoel, J. Phys. E: Sci. Instrum. 17 (1984) 896.
[12] M. McClain, A. Feldman, D. Kahaner, X. Ying, Comput. Phys. 5 (1991) 45.
[13] T. Kawaguchi, K. Masui, Jpn. J. Appl. Phys. 26 (1987) 15.
[14] S.H. Wemple, M. DiDomenico Jr., Phys. Rev. B 3 (1971) 1338.
[15] S.H. Wemple, Phys. Rev. B 7 (1973) 3767.
[16] J. Tauc, in: J. Tauc (Ed.), Amorphous and Liquid Semiconductors, Plenum, New York, 1974, p. 159.
[17] J. Kerr, in: D.R. Lide (Ed.), Chemical Rubber Company Handbook of Chemistry and Physics, 77th Ed., CRC, Florida, 1996.
[18] J.A. Van Vechten, Phys. Rev. 182 (1969) 891.
[19] T.I. Kosa, T. Wagner, P.J.S. Ewen, A.E. Owen, Philos. Mag. B 71 (1995) 311.
[20] A. Fisher-Colbrie, A. Bienenstock, P.H. Fuoss, M.A. Marcus, Phys. Rev. B 38 (1988) 12388.
[21] T. Wagner, Mir. Vlcek, S.O. Kasap, Mil. Vlcek, M. Frumar, J. Non-Cryst. Solids 284 (2001) 168.